LETTER TO THE EDITOR

On the theory of anomalous elastic properties of disordered Al–Li and Al–Mg alloys

V G Vaks and N E Zein

I V Kurchatov Institute of Atomic Energy, Moscow 123182, USSR

Abstract. Calculations of the electronic structure, equilibrium volume Ω_e and elastic constants C_{ij} for the disordered $Al_{1-x}Li_x$ and $Al_{1-x}Mg_x$ alloys have been performed. We use the virtual crystal approximation, first-principles pseudopotentials and the previously discussed method of calculating C_{ij}, based on the density functional approach. The results describe fairly well all the peculiar features of the $C_{ij}(x)$ and $\Omega_e(x)$ dependences in these alloys and show that the anomalies in these dependences are due to the band structure effects.

The unusual atomic properties of the disordered $Al_{1-x}Li_x$ alloys attract great attention. Lithium is a much softer and less dense metal than aluminium: its shear modulus, G, and Young modulus, E, are 4–5 times as small, while the atomic volume, Ω, is 30% larger than those in Al. Nevertheless, the addition of Li to Al (in the solubility region $x \lesssim 0.14$) results in a significant increase in G and E [1, 2] as well as in a contraction (rather than expansion) of the lattice [3, 4], while the bulk modulus B decreases monotonically [2–4]. This increase of G (combined with other favourable properties) makes the Al–Li alloys highly interesting for technological applications [1, 2], which, in its turn, stimulates attempts to understand their unusual behaviour [1–4]. In particular, Noble *et al* [1] supposed that the increase in G is related to some changes in the electronic structure of the alloys but, apparently, there are no available microscopic considerations yet. In the Al–Mg system, analogous anomalies are much less pronounced and manifest only in a very slow decrease of $E(x)$ with increasing x_{Mg} [5].

At the same time, the possibility of anomalous variations of shear constants $C_{ss'}$ in metals under certain changes in band structure were recently discussed by a number of authors [6–10]. It is mentioned, in particular, that the $C_{ss'}$ values can increase (decrease) sharply when the Fermi level ε_F approaches the sharp minimum (maximum) point in the electron state density $n(\varepsilon)$ [8] and these effects appear to be displayed clearly in peculiar concentration dependences of $C_{ss'}$ in some BCC transition metal alloys [6, 7], as well as in anomalous pressure dependences of $C_{ss'}$ for a number of alkali and alkaline earth metals [9, 10]. Since calculations of $n(\varepsilon)$ for Al seem to indicate the presence of the minimum in $n(\varepsilon)$ near and below ε_F [11, 12], it is natural to suppose that the anomalous $C_{ss'}(x)$ dependences in $Al_{1-x}Li_x$ and $Al_{1-x}Mg_x$ are connected with ε_F approaching the relevant minimum points of $n(\varepsilon)$ in the alloys.

The treatments carried out in other works [6–10] were, mainly, qualitative and used simplified models. The consistent method for calculating $C_{ss'}$ in metals, based on the

density functional approach, was proposed in [13]. Its efficiency and accuracy were demonstrated by calculations of C_{ij} for Nb, Mo and also for Ca and Al [14]. To apply this method to a disordered alloy, one should use additional approximations, e.g. that of the virtual crystal (VCA), in which the $A_{1-x}B_x$ alloy is described as a metal with the average pseudopotential $V = (1 - x)V_A + xV_B$. However, one may believe that it suffices to employ the VCA for elucidation of the main features of the concentration dependences under consideration, while the character of errors brought about by this approximation is qualitatively clear (see below).

In the present paper we apply the VCA and methods used in other works [13, 14] to the first-principles calculation of the electronic structure, equilibrium volume and elastic constants in the disordered alloys $Al_{1-x}Li_x$ and $Al_{1-x}Mg_x$. Let us present the main relations.

The expressions for the elastic constant C_{ij} in a monatomic crystals (neglecting phonon and temperature effects) can be written as [13]

$$C_{ij} = (1/N)(\partial^2 E/\partial u_i \partial u_j) = C_{ij}^{\text{Mad}} + C_{ij} + C_{ij}^{\text{b}} + C_{ij}^{\text{ee}}. \tag{1}$$

Here E and N are the total energy and number of atoms, u_i is the homogeneous strain (in the Voigt notation), C_{ij}^{Mad} is the 'Madelung' term, i.e. the elastic constant of the point-ion lattice in the homogeneous compensating charge, and C_{ij}^{np} is the contribution to C_{ij} which arises due to the non-point-like character of ions [15]

$$C_{ij}^{\text{Mad}} = b_{ij} Z_e^2/\Omega^{4/3} \qquad C_{ij}^{\text{np}} = (1/\Omega) \lim (V(q, q) + 4Ze^2/\Omega q^2)_{q \to 0} \tag{2}$$

where b_{ij} denotes numerical coefficients determined only by the lattice geometry (see e.g. [10]); $V(q_1, q_2)$ is the Fourier component of the non-local pseudopotential V, and Z is the ion valency. The term C_{ij}^{b} in (1) corresponds to the band-structure energy contribution and is equal to a sum of contributions of the electronic states on the Fermi surface C_{ij}^{FS}, and those in the Fermi volume, C_{ij}^{FV}:

$$C_{ij}^{\text{FS}} = -\frac{1}{N\Omega} \sum_{\nu} \delta(\xi_\nu) \left[\frac{\partial \xi_\nu}{\partial u_i} \left(\varphi_\nu \frac{\partial \hat{H}_e}{\partial u_j} \varphi_\nu \right) + \frac{\partial \xi_\nu}{\partial u_j} \left(\varphi_\nu \frac{\partial \hat{H}_e}{u_i} \varphi_\nu \right) \right] \tag{3a}$$

$$C_{ij}^{\text{FV}} = \frac{1}{N\Omega} \sum_{\nu} \theta(-\xi_\nu) \left[\left(\varphi_\nu \frac{\partial^2 H_e}{\partial u_i \partial u_j} \varphi_\nu \right) + \left(\varphi_\nu \frac{\partial \hat{H}_e}{u_i} \frac{\partial \varphi_\nu}{\partial u_j} \right) + \left(\varphi_\nu \frac{\partial \hat{H}_e}{\partial u_j} \frac{\partial \varphi_\nu}{\partial u_i} \right) \right]. \tag{3b}$$

Here $\xi_\nu = \varepsilon_\nu - \varepsilon_F$, ε_ν and φ_ν are the energy and the wave function of the state ν; $\hat{H}_e$ is the Hamiltonian for an electron in the ion lattice (without the electron–electron interaction term V_{ee}); $(\varphi \hat{A} \psi)$ is the matrix element of the operator $\hat{A}$ between the states φ and ψ; while $\theta(x)$ is the step function equal to zero at $x < 0$ and unity at $x > 0$. The last term in (1), $C_{ij}^{\text{ee}} = C_{ij}^{\text{xc}} + C_{ij}^{\text{dC}}$, corresponds to the corrections for double counting of the V_{ee} contributions to C_{ij}^{b} and consists of two terms, the exchange–correlation contribution, C_{ij}^{xc}, and the direct Coulomb one, C_{ij}^{dC}

$$C_{ij}^{\text{xc}} = \int d^3r \, \rho(r) \left[(\varepsilon_{\text{xc}} - \mu_{\text{xc}}) \frac{1}{\Omega} \frac{\partial^2 \Omega}{\partial u_i \partial u_j} - \frac{1}{2} \left(\delta_{ih} \frac{\partial \mu_{\text{xc}}}{\partial u_j} + \delta_{jh} \frac{\partial \mu_{\text{xc}}}{\partial u_i} \right) \right] \tag{4a}$$

$$C_{ij}^{\text{dC}} = 2\pi e^2 \sum_{g \neq 0} \left[n_g^2 \frac{\partial^2}{\partial u_i \partial u_j} \left(\frac{1}{\Omega g^2} \right) + n_g \frac{\partial n_g}{\partial u_i} \frac{\partial}{\partial u_j} \left(\frac{1}{\Omega g^2} \right) + n_g \frac{\partial n_g}{\partial u_j} \frac{\partial}{\partial u_i} \left(\frac{1}{\Omega g^2} \right) \right]. \tag{4b}$$

Here $\rho(r)$ is the electron density; $\varepsilon_{\text{xc}}(\rho)$ is the exchange–correlation energy for the homogeneous electron gas; $\mu_{\text{xc}} = \partial \varepsilon_{\text{xc}}/\partial \rho$; $\delta_{ih} = \delta_{i1} + \delta_{i2} + \delta_{i3}$, the integral in (4a) is taken over the elementary cell; g is the reciprocal lattice vector; and $n_g = \Omega \rho_g$, where ρ_g is the Fourier component of $\rho(r)$.
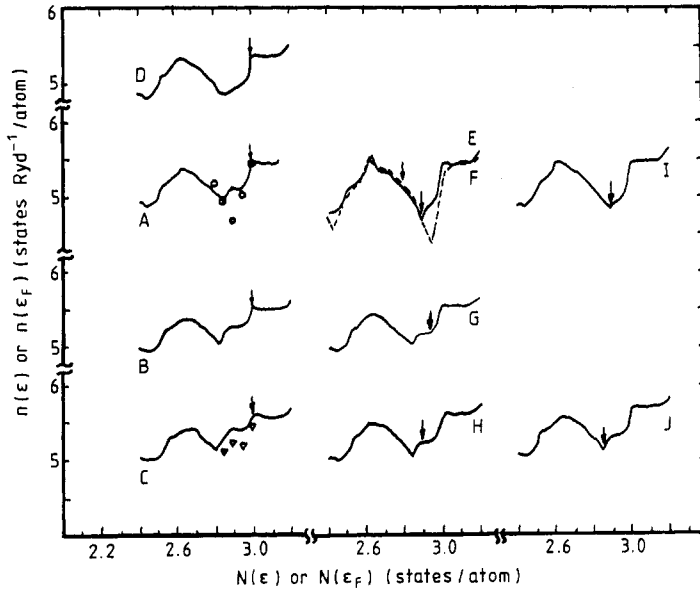
Figure 1. Curves: the density of electronic states, $n(\varepsilon)$, in the vicinity of the Fermi level ε_F versus the number of states, $N(\varepsilon)$. Curves A, B, C and D correspond to pure Al at Ω/Ω_0 values equal to 1, 1.02, 1.04 and 0.98; E and F, $Al_{1-x}Li_x$ alloys at $x = 0.05$ and $x = 0.1$; G, H and J, $Al_{1-x}Mg_x$ alloys with $\Omega = \Omega_0(1 + 0.4x)$ at $x = 0.05, 0.1$ and 0.15; I, $Al_{0.9}Mg_{0.1}$ alloy with $\Omega = \Omega_0$. The arrow at the curve indicates the $n(\varepsilon_F)$ value. Open symbols show values of $n(\varepsilon_F)$ versus $N(\varepsilon_F)$ for various alloys; circles correspond to $Al_{1-x}Li_x$ alloys; triangles, $Al_{1-x}Mg_x$ alloys with $\Omega = \Omega_0(1 + 0.4x)$.

In calculations we employed the first-principles norm-conserving pseudopotentials of Bachelet *et al* [16] and the expression for $\varepsilon_{xc}(\rho)$, proposed by Perdew and Zunger [17]. We used the basis of 137 plane waves in the FCC lattice and took 531 k-points in the integration over the $1/48$ irreducible part of the Brillouin zone (BZ) with quadratic interpolation between them. The self-consistent procedure for finding the electron–electron interaction V_{ee} and other computational details are described in [14]. For the atomic volume Ω in the Al–Li alloys, we took the value $\Omega = \Omega_0 = 110.6$ au (corresponding to pure Al at $T = 0$ [4]), neglecting the previously mentioned small concentration contraction $d \ln \Omega/dx = -(3\text{–}5) \times 10^{-2}$ [3, 4]. In the $Al_{1-x}Mg_x$ alloys, the contraction expansion $d \ln \Omega/dx \simeq 0.4$ is noticeable [1, 18], and we have taken it into account.

The results of the calculations are presented in figures 1, 2 and tables 1–3. Let us firstly discuss the electron state density $n(\varepsilon)$ near ε_F, which is presented in figure 1 versus the number of states in the valence band, $N(\varepsilon)$

$$N(\varepsilon) = \int_{-\infty}^{\varepsilon} n(\varepsilon') \, d\varepsilon'. \tag{5}$$

The ε_F values (counted off from the mean value of the pseudopotential, $V(0,0)$ [13]) are presented in tables 2 and 3.

Figure 1 illustrates variations in $n(\varepsilon)$ with volume Ω and concentration x in the alloys considered. Curves A, B, C and D show that the Ω-dependence of $n(\varepsilon)$ is, generally, not strong. On the contrary, the change of $n(\varepsilon)$ with x in $Al_{1-x}Li_x$ alloys is very sharp (unlike in the rigid-band model) and its drop at $N = 2.9$–2.95 sharpens significantly with

Table 1. Contributions to pressure p and moduli B_{ij} in Al.

Quantity	Experiment [18]	Calculation					
		Total	Mad	np	b	xc	dC
P	0	−2.0	−240.1	204.4	98.2	−64.8	0.3
B	79.4	74.4	−320.2	408.8	70.0	−84.9	0.7
B_{33}	26.3	25.9	16.6	0	11.0	0	−1.8
B_{44}	31.7	26.2	149.0	0	−123.3	0	0.5
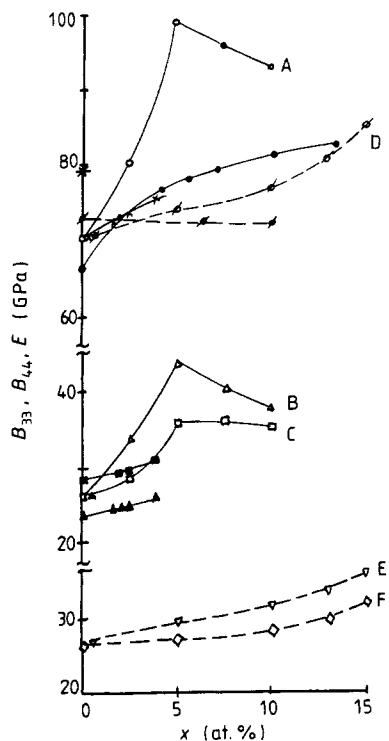
Figure 2. Concentration dependence of elastic moduli in the Al–Li and Al–Mg alloys. Open symbols correspond to calculations, full symbols and crosses, to experiments (curves link the symbols as a guide to the eye). The curves A, B and C (D, E and F) correspond to the values of E, B_{33} and B_{44} calculated for $Al_{1-x}Li_x$ ($Al_{1-x}Mg_x$) alloys. Experimental data: circles denote $E(x)$ for polycrystal $Al_{1-x}Li_x$[1]; crosses, $E(x)$ for single-crystal $Al_{1-x}Li_x$ [2]; crossed-circles, $E(x)$ for polycrystal $Al_{1-x}Mg_x$ [5]; triangles, $B_{33}(x)$ for $Al_{1-x}Li_x$ [2]; squares, $B_{44}(x)$ for $Al_{1-x}Li_x$ [2]; asterisk, E for single-crystal Al at $T = 0$ [18, 19].

rising x. The point of this drop, ε_c, corresponds to the states in the third band near the point K (or U) of the BZ, and at $x \simeq 0.05$ the Fermi level ε_F reaches this point. The analysis shows that the enhancement of the $n(\varepsilon)$ singularity at $\varepsilon = \varepsilon_c$ is, mainly, connected with the flattening of the dispersion curves $\varepsilon_\nu = \varepsilon_n(p)$ near the K point and K–W line. For example, at $x = 0$, 0.05, and 0.1, values of $\varepsilon_c = \varepsilon_3(K)$ are: 726, 734, and 741 mRyd, while the $\varepsilon_3(W)$ ones are 765, 759, and 751 mRyd, respectively. Thus, the difference $\Delta_3^{WK} = \varepsilon_3(W) - \varepsilon_3(K)$ drops by a factor of four. These variations in $\varepsilon_n(p)$ are, in their turn, mainly determined by changes of the matrix elements $\langle p | \tilde{V} | p + g \rangle$ of the effective pseudopotential $\tilde{V} = V + V_{ee}$ corresponding to $g = (1,1,1)$ and states $|p\rangle$ and $|p + g\rangle$ near points K and U: from $x = 0$ to $x = 0.1$ the elements $\langle K | \tilde{V} | U \rangle$ rise from 71 to 78 mRyd, while for example, the elements $\langle W | \tilde{V} | W' \rangle$ with $g = (2,0,0)$ for $|p\rangle$ states near the W points change twice as slowly, from 119 to 125 mRyd.

In $Al_{1-x}Mg_x$ alloys the $n(\varepsilon)$ changes with x are much weaker (when the concentration expansion is taken into account). For example, from $x = 0$ to $x = 0.1$ the Δ_3^{WK} difference

Table 2. Calculated values of p, B_{ij}, ε_F and $n(\varepsilon_F)$ for alloys $Al_{1-x}Li_x$.

x (%)	p	B		B_{33}					B_{44}					ε_F (mRyd)	$n(\varepsilon_F)$ (Ryd^{-1}/atom)
		Total	FS	Total	FS	NFS	FV	Mad	Total	FS	NFS	FV	Mad		
0	−2.0	74	−3	26	−104	130	115	17	26	−92	118	−31	149	755	5.46
2.5	−2.3	74	−3	33	−90	123	109	16	28	−87	115	−29	144	744	5.04
5	−2.7	75	−1	44	−77	120	106	16	36	−78	113	−26	139	732	4.69
7.5	−2.9	74	−1	40	−80	120	106	15	36	−78	113	−21	134	720	4.96
10	−3.1	73	−1	38	−82	119	106	15	35	−78	112	−17	130	708	5.17

Table 3. Calculated values of p, B_{ij}, ϵ_F and $n(\epsilon_F)$ for alloys $Al_{1-x}Mg_x$.

x (%)	Ω/Ω_0	p	B		B_{33}					B_{44}					ϵ_F (mRyd)	$n(\epsilon_F)$ (Ryd^{-1}/atom)
			Total	FS	Total	FS	NFS	FV	Mad	Total	FS	NFS	FV	Mad		
0	1	-2	74	-3	26	-104	130	115	17	26	-92	118	-31	149	755	5.46
5	1.02	-3	70	-3	29	-92	122	108	16	27	-86	113	-28	140	737	5.20
10	1.04	-3	65	-2	31	-84	116	102	15	28	-80	108	-25	132	719	5.25
15	1.06	-4	63	-1	36	-79	111	99	14	32	-72	104	-21	124	701	5.12
10	1.033	-3	68	-2	33	-84	116	103	15	30	-80	109	-24	133	722	5.20
10	1	-1	79	-2	41	-79	120	106	16	38	-81	118	-21	139	736	4.87

decreases only by 5% (both the $\langle K | \bar{V} | U \rangle$ and $\langle W | \bar{V} | W' \rangle$ elements decrease by approximately 4%). Therefore, the $n(\varepsilon)$ functions for $x = 0$–0.15, shown by curves A, G, H and J in figure 1, are rather similar, and ε_F reaches the point of singularity ε_c at $x \simeq 0.15$. Let us note that in the absence of the expansion, i.e. if $\Omega(x) = \Omega_0 = $ constant, the form of $n(\varepsilon)$ noticeably changes with x, and $n(\varepsilon)$ has a significant singularity at $x \simeq 0.11$ (see curve I in figure 1).

The results for pressure and elastic constants are shown in tables 1–3 and in figure 2. Instead of the Voigt constants C_{ij}, we present the Fuchs-type moduli B_{ij} which have a clearer meaning of the bulk modulus B and shear constant B_{33} or B_{44}, including the case of non-zero pressure $p \neq 0$ [20]:

$$B_{11} = B = \tfrac{1}{3}(C_{11} + 2C_{12} + p)$$

$$B_{33} = \tfrac{1}{2}(C_{11} - C_{12}) - p$$

$$B_{44} = C_{44} - p. \tag{6}$$

The theoretical equilibrium volume Ω_e is connected with the calculated $p = p(\Omega)$ as $\Omega_e = \Omega(1 + p/B)$. The NFS contribution to the shear constants B_{ss} in tables 2 and 3 is defined as the difference between the total B_{ss} and the Fermi surface contribution to it:

$$B_{ss}^{NFS} = B_{ss} - B_{ss}^{FS} = B_{ss}^{FV} + B_{ss}^{Mad} + B_{ss}^{dC} \tag{7}$$

where we allow for $B_{ss}^{ns} = B_{ss}^{xc} = 0$. In the evaluation of the Young modulus $E = 3G(1 + G/3B)^{-1}$, the values of the 'averaged' shear constant G estimated according to Voigt, $G_V = \tfrac{1}{5}(2B_{33} + 3B_{44})$, and Reuss, $G_R = 5(2/B_{33} + 3/B_{44})^{-1}$ [21], coincide within a per cent, and so we take $G = \tfrac{1}{2}(G_R + G_V)$. Values of p, B_{ij} and E are given in GPa everywhere.

Table 1 shows the results for pure Al. To compare the calculated p with experiment, one has to add the phonon contribution p_{ph} to its value in table 1. According to the estimate [22], p_{ph} is about 0.9 at $T = 0$. Then the calculated volume Ω_e differs from the observed one only by 1.5%. The calculated B_{ij} also agree well with the experiment. This shows the sufficient accuracy of the first-principles methods used for pure Al. Table 1 also shows that contributions B_{ij}^{dC} of the Coulomb interaction of the inhomogeneous components of the electron density $\rho(r) - \langle \rho \rangle$ are small in Al (as well as in the Al–Li and Al–Mg systems) which seems to be natural for 'nearly-free-electron' metals. Thus, the shear constant values are determined practically only by the 'band' and Madelung contributions.

Figure 2 displays vivid manifestations of the 'band' effects in the shear constants of the alloys considered. In accordance with the aforementioned general considerations [8], the closeness of ε_F to the sharp minimum points of $n(\varepsilon)$ results in the steep rise of the calculated $B_{ss}(x)$ and $E(x)$ in $Al_{1-x}Li_x$ near $x = 0.05$. Even so, the rise of $B_{33}(x)$ noticeably exceeds that of $B_{44}(x)$, which agrees qualitatively with experiments [2]. At the same time the calculated bulk modulus (table 2) varies slowly with x, in accordance with its weak sensitivity to the band effects under consideration [8] (in the experiment [2] d ln B/d$x \simeq -0.8$). The p-values in table 2 reveal a tendency to contraction with rising x, and the calculated (d ln Ω/dx) value is even 3–5 times as great as the observed one [3, 4]. In the $Al_{1-x}Mg_x$ alloys, where the drop in $n(\varepsilon)$ with x is much weaker, the calculated $B_{ss}(x)$ and $E(x)$ values increase rather slowly at $x \lesssim 0.13$, $B(x)$ monotonically decreases, and $p(x)$ implies a concentration expansion (though being approximately one-third of the observed one [1, 18]). Near $x_c \simeq 0.15$, where ε_F reaches ε_c, the calculations again show some band rise of $B_{ss}(x)$ and $E(x)$. However, here the singularity in $n(\varepsilon)$ is much weaker than that in the Al–Li case. Thus, the possibility of

its smearing and weakening in real alloys seems to be much more probable. Therefore, the calculations correctly describe all the qualitative features of the $B_{ij}(x)$ and $\Omega_c(x)$ dependences in the alloys considered, while the quantitative disagreements with experiments may be connected with the disregarded effects discussed below.

Tables 2 and 3 also illustrate the importance of different contributions to the band anomalies of $B_{ss}(x)$. In accordance with the considerations in [8–10], these anomalies are, mainly, determined by the Fermi surface contribution B_{ss}^{FS}, while the rest of the terms vary smoothly and monotonically with x. The two bottom lines of table 3 illustrate the effects of the concentration expansion on $B_{ij}(x)$ in $Al_{1-x}Mg_x$. The comparison of the third and fifth lines shows that slight changes in Ω (corresponding, in particular, to different experimental data, [1] and [18]) have little effect on B_{ij}. However, the total absence of the expansion (line 6) would result in a sharp band rise of $B_{ss}(x)$ near $x \simeq 0.1$ in accordance with the above-mentioned closeness of ε_F to the strong singularity point in $n(\varepsilon)$.

To compare the calculations with experiments, one should take into account that in the VCA employed we disregard the effects of smearing of the band singularities considered due to non-conservation of the electron quasimomentum in a disordered alloy and the resulting smearing of the BZ and the FS. Though the theoretical [23] and experimental [24, 25] estimates show that in a number of alloys such a smearing is not large, in principle, it must smooth over all the singularities in $n(\varepsilon)$ and the related anomalies in the physical properties. This can be particularly true for such strong singularities as those for Al–Li alloys in figure 1 (the scale of smoothing can be estimated, for example, employing the coherent potential approximation for $n(\varepsilon)$). The weakening of the singularities (i.e. the sharpness of the band maximum in the structural stability at $\varepsilon_F = \varepsilon_c$) should evidently decrease the values of B_{ss}, B and the rise of the cohesion, i.e. of the tendency towards system contraction, thereby bringing all the above theoretical results closer to the observed ones. In addition, a part of the deviations from experiment can be due to the disregarded phonon and temperature effects, as well as to the imperfection of the alloys investigated, i.e. the presence of defects and impurities there. For example, the E-value for single-crystal Al at $T = 0$ [18] noticeably exceeds those for poly-crystal Al at room temperature T_r [1, 5], see figure 2. Note also that a 'break' in the $E(x)$ dependence for $Al_{1-x}Li_x$ seen in experiments [1], corresponds to the values $x \simeq 0.03$ at which the maximum corrosion resistance has also been observed [18]. This might imply that for these real alloys the critical point $\varepsilon_F = \varepsilon_c$ corresponds to $x_c^{exp} \simeq 0.03$ rather than to $x_c \simeq 0.05$, as in our calculations.

Let us now remark on the estimates of C_{ij} for the ordered δ' phase, Al_3Li, of [2]. At the experimental $T \geqslant T_r$, the δ' phase precipitates out of the disordered α phase at $x \geqslant x_\alpha \simeq 0.05$. To estimate $C_{ij}^{\delta'}$ from the measured C_{ij}^m in the two-phase region, Müller *et al* [2] used the relation

$$C_{ij}^m = (1 - f)C_{ij}^\alpha + fC_{ij}^{\delta'} \qquad (8)$$

where f is the volume of the δ' phase. The values $C_{ij}^\alpha = C_{ij}^\alpha(x, T)$ at the equilibrium curve $T = T_{\alpha-\delta'}(x)$ in (8) were obtained by the x- and T-linear extrapolation from the values measured at $x \leqslant 0.04$. However, the values of $C_{ij}^{\delta'}(T)$ found show an extremely sharp temperature dependence, about five times as strong as that measured in the α phase. This seems to be very strange, and even more so since the moduli themselves increase with ordering, $C_{ij}^{\delta'} > C_{ij}^\alpha$, and thus the lattice stiffens. One may suppose that this sharp dependence of $C_{ij}^{\delta'}$ on T is actually spurious and was obtained only due to the unjustified x-linear extrapolation for $C_{ij}^\alpha(x)$ in (8). Indeed, if the rise of B_{ss} with x is due

to the band-structure effects discussed above, then at $x > x_c \simeq 0.05$ the rise must slow down and the slope of the $B_{ss}(x)$ curves must decrease. Thus at large T, the $C_{ij}^{\alpha}(x, T)$ values on the curve $T_{\alpha-\delta'}(x)$ should decrease, while $C_{ij}^{\delta'}$ (found from (8)) should increase as compared with the estimates made in [2]. This must diminish the sharp drop of $C_{ij}^{\delta'}$ with T, obtained by Müller *et al* [2]. Let us also note that the solubility limit for $Al_{1-x}Li_x$ alloys at $T \sim T_r$, $x_{\alpha}^{Li} \simeq 0.05$, as well as that for $Al_{1-x}Mg_x$ alloys at high T, $x_{\alpha}^{Mg} \simeq 0.18$ [18], are close to the critical values discussed above, $x_c^{Li} \simeq 0.05$, $x_c^{Mg} \simeq 0.15$, corresponding to the equality $\varepsilon_F = \varepsilon_c$. This can reflect the maximum band stability of the disordered α phase at these points.

To conclude, the unusual concentration dependences of $B_{ij}(x)$ and $\Omega(x)$ in the $Al_{1-x}Li_x$ and $Al_{1-x}Mg_x$ alloys are, apparently, explained by the band-structure effects discussed above, and the calculations presented describe all the qualitative features of these dependences. To verify and specify these considerations, further experimental investigations of these alloys are obviously desirable, in particular, low-temperature measurements of thermopower, specific heat and thermal expansion [23–25, 8], as well as direct measurements of $B_{ss}(x)$ in the α phase of $Al_{1-x}Li_x$ at $x \geqslant 0.05$.

References

[1] Noble B, Harris S J and Dinsdale K 1982 *J. Mater. Sci.* **17** 461
[2] Müller W, Bubeck E and Gerold V 1986 *Aluminium–Lithium Alloys* vol III, ed C Baker *et al* (London: Institute of Metals) p 435
[3] Podloucky R, Jansen H J F, Guo O Q and Freeman A J 1988 *Phys. Rev.* B **37** 5478
[4] Solt G and Werner K 1981 *Phys. Rev.* B **24** 817
[5] Köster W and Rauscher W 1948 *Z. Metallkd.* **39** 111
[6] Bujard P, Sanjines R, Walker E, Ashkenazi J and Peter M 1981 *J. Phys. F: Met. Phys.* **11** 775
[7] Ohta Y and Shimizu M 1983 *J. Phys. F: Met. Phys.* **13** 761
[8] Vaks V G and Trefilov A V 1983 *Pis. Zh. Eksp. Teor. Fiz.* **38** 373; 1988 *J. Phys. F: Met. Phys.* **18** 213
[9] Vaks V G, Katsnelson M I, Koreshkov V G, Likhtenstein A I, Parfenov O E, Skok V F, Sukhoparov V A, Trefilov A V and Chernyshov A A 1989 *J. Phys.: Condens. Matter* **1** 5319
[10] Vaks V G, Katsnelson M I, Likhtenstein A I, Peschanskikh G V and Trefilov A V 1990 *J. Phys.: Condens. Matter* submitted
[11] Grechnev G E, Svechkarev I V and Ushakova N V 1986 *Fiz. Metall. Metalloved.* **62** 202
[12] Papaconstantopoulos D A 1986 *Handbook of the Band Structure of Elemental Solids* (London: Plenum)
[13] Zein N E 1984 *Fiz. Tverd. Tela* **28** 3028
[14] Zein N E, Kamyshenko V V and Samolyuk G D 1990 *Fiz. Tverd. Tela* at press
[15] Brovman E G and Kagan Yu M 1974 *Lattice Dynamics* ed A A Maradudin and G K Horton (Amsterdam: North-Holland)
[16] Bachelet G B, Hamann D R and Schlüter M 1982 *Phys. Rev.* B **26** 4199
[17] Perdew J P and Zunger A 1981 *Phys. Rev.* B **23** 5048
[18] Vol A E 1959 *Structure and Properties of Binary Metallic Systems* (Moscow: Fizmatgiz)
[19] Kamm G N and Alers G A 1964 *J. Appl. Phys.* **35** 327
[20] Brovman E G, Kagan Yu M and Kholas A 1970 *Fiz. Tverd. Tela* **12** 1001
[21] Hirth J P and Lothe J 1968 *Theory of Dislocations* (New York: Wiley) ch 13
[22] Kravchuk S P 1975 *Thesis* (Moscow: IAE)
[23] Vaks V G, Trefilov A V and Fomichev S V 1981 *Zh. Eksp. Teor. Fiz.* **80** 1613
[24] Egorov V S and Fedorov A I 1983 *Zh. Eksp. Teor. Fiz.* **85** 1647
[25] Bashkatov N V and Sorokin N L 1989 *Fiz. Tverd. Tela* **31** 326